"Study of the interaction between the G-quadruplex-forming thrombin-binding aptamer and the porphyrin 5,10,15,20-tetrakis-(N-methyl-4-pyridyl)-21,23H-porphyrin tetratosylate" Del Toro, M., Gargallo, R., Eritja, R., Jaumot, J. Anal. Biochem., 379(1), 8-15 (2008). doi: 10.1016/j.ab.2008.04.044

Study of the interaction between the G-quadruplex-forming thrombin-binding aptamer and the porphyrin 5,10,15,20-tetrakis-(N-methyl-4-pyridyl)-21,23H-porphyrin tetratosylate.

Miquel del Toro[1], Raimundo Gargallo[1], Ramon Eritja[2] and Joaquim Jaumot[1*]

1. *Department of Analytical Chemistry, Universitat de Barcelona, Diagonal 647, Barcelona, E-08028 Spain.*
2. *Department of Structural Biology, IBMB-CSIC, Jordi Girona 18-34, Barcelona, E-08034 Spain*

* Author to whom correspondence should be addressed

Tel: +34-934034445

Fax: +34-934021233

E-mail: joaquim@apolo.qui.ub.es

Abstract

The G-quadruplex DNA structure has been suggested to be a potential target for anticancer therapies. Therefore, there is increasing interest in the development of drugs that could modulate the stability of G-quadruplex structures. In the current work, the interaction between the thrombin-binding aptamer (TBA, 5'-GGT TGG TGT GGT TGG-3'), which can form an intramolecular G-quadruplex structure, and the porphyrin 5,10,15,20-*tetrakis*-(*N*-methyl-4-pyridyl)-21,23H-porphyrin tetratosylate (TmPyP4) was studied. The application of a high-performance liquid chromatography–photodiode array (HPLC–PDA) detector-based method to study this kind of interaction was tested. Molecular absorption data recorded along the chromatographic runs were analyzed by means of multivariate data analysis methods. Moreover, biospecific interaction analysis (BIA) by surface plasmon resonance (SPR) and melting and mole ratio experiments monitored by UV–visible molecular absorption and circular dichroism spectroscopies, were applied to confirm and expand the chromatographic studies. The results showed the formation of an interaction complex with a stoichiometry 1:1 (TmPyP4/TBA) and logarithm of the equilibrium constant equal to 5.7 ± 0.2. Melting and circular dichroism data reflected that the initial G-quadruplex structure of TBA is stabilized in the interaction complex, being slightly distorted by the presence of the ligand.

[1]Abbreviations used: TBA, thrombin-binding aptamer; SPR, surface Plasmon resonance; HPLC, high-performance liquid chromatography; TmPyP4, 5,10,15,20- tetrakis-(N-methyl-4-pyridyl)-21,23H-porphyrin tetratosylate; PDA, photodiode array; BIA, biospecific interaction analysis; CD, circular dichroism; PAGE, polyacrylamide gel electrophoresis; NMR, nuclear magnetic resonance; ESI–MS, electrospray ionization–mass spectrometry; TEAA, triethylammonium acetate; SA, streptavidin; Hepes, 4-(2-

hydroxyethyl)-1-piperazineethanesulfonic acid; MCR–ALS, multivariate curve resolution by alternating least squares; PBS, phosphate-buffered saline.

Keywords: *G-Quadruplex, porphyrins, DNA-drug interaction, chromatography, chemometrics*

Introduction

Guanine bases can associate in a cyclic arrangement to form planar arrangements of four guanines, known as G-quartets, in which each guanine is bonded to two neighboring bases via hydrogen bonds. These G-quartets enable DNA sequences rich in guanines to form complex folded structures, known as G-quadruplexes, which are further stabilized by cations. The biological relevance of G-quadruplexes is now being investigated intensively, largely as a consequence of the identification of G-quadruplexforming sequences in the genome (e.g., telomeres, several oncogenes and aptamers) [1–3]. Aptamers are oligonucleotide or peptide molecules that bind a specific target molecule [4–6]. The thrombin-binding aptamer (TBA)[1] constitutes the first example of in vitro selection of DNA oligonucleotides targeted toward a protein that has no known physiological binding to nucleic acids [7,8]. For this reason, and because of their potential importance as anticlotting therapeutics, TBA has been studied extensively. TBA aptamer, whose sequence is 50-GGT TGG TGT GGT TGG-30 (Scheme 1), adopts an intramolecular antiparallel G-quadruplex structure in the presence of K^+ ions [9–11]. Recently, the use of cationic porphyrins as modulator agents in the aptamer's function in blood clotting was proposed [12].

Several instrumental techniques have been used to monitor the interactions between G-quadruplexes and ligands, ranging from classical techniques of analysis such as molecular spectroscopies (molecular absorption, fluorescence, or circular dichroism) to modern techniques that allow monitoring molecular reactions in real time by surface plasmon resonance (SPR) [13–16]. However, to the best of our knowledge, chromatographic techniques still have not been applied to monitor the interactions between G-quadruplexes and ligands. This could be due to the difficulties inherent in the analysis of oligonucleotides that show complex secondary structures at low temperatures. In this case, broad and poorly defined peaks are usually obtained. On the other hand, analysis of porphyrins by means of high-performance liquid chromatography.

(HPLC) methods has been studied extensively in the literature, but only for quantitative purposes in environmental or biomedical samples [17–20].

In this work, the study of the interaction between TBA and 5,10,15,20-*tetrakis*-(*N*-methyl-4-pyridyl)-21,23H-porphyrin tetratosylate (TmPyP4) has been studied (Scheme 1). The competence of an HPLC–photodiode array (PDA) detector to detect and quantify the interaction of G-quadruplexes with ligands was tested with TBA and TmPyP4. This interaction was also studied by means of a biospecific interaction analysis (BIA) by SPR and melting and mole ratio experiments monitored by UV–visible molecular absorption and circular dichroism (CD) spectroscopies.

Experimental

Reagents

The oligonucleotide sequence TBA (5'-GGT TGG TGT GGT TGG-3') and the biotinilated TBA sequence TBA-Bio (5'-GGT TGG TGT GGT TGG-B-3') were synthesized on an Applied Biosystems 3400 DNA synthesizer (Applied Biosystems, Foster city, CA, USA) using the 200 nmols scale synthesis cycle. Biotin (B) was introduced at the 3'-end using the controlled pore glass functionalized with a tetraethyleneglycol derivative of biotin (3'-Biotin-TEG CPG, Link Technologies, Lanarkshire, UK). Standard phosphoramidites were used for the natural bases. Ammonia deprotection was performed overnight at 55 ºC. The resulting products were desalted by Sephadex G-25 (NAP-10, Amersham Biosciences, Piscataway, NJ, USA) and used without further purification. The length and homogeneity of the oligonucleotides was checked by denaturing polyacrylamide gel electrophoresis (PAGE) and reversed-phase HPLC using X-Terra® columns. DNA concentration was determined by absorbance measurements (260 nm) at 90 ºC considering an extinction coefficient of 147,300 according to the nearest-neighbour approximation as implemented in Oligo Parameter Calculation (http://proligo2.proligo.com/Calculation/calculation.html). Prior to their use, samples were heated at 90 ºC for 5 minutes and allowed to renaturalize, cooling slowly until room temperature. Oligonucleotide samples were kept overnight at 4 ºC until their use.

TmPyP4 porphyrin (Scheme 1B) was purchased from Porphyrin Systems (Lübeck, Germany). Stock solutions were prepared by dissolving the solid reagent in the appropriate volume of ultrapure water (Millipore, Billerica, MA, USA). The purity of TmPyP4 was checked by means of nuclear magnetic resonance (NMR) and electrospray ionization-mass spectrometry (ESI-MS) (see Supplementary material)

Diluted solutions for measurements were prepared in ultrapure water (Millipore, Billerica, MA, USA). Other reagents used in this work were KCl (Merck, Germany), $MgCl_2$ (Merck, Germany), the buffer compounds Na_2HPO_4 Panreac, Spain) and KH_2PO_4 (Panreac, Spain), NaOH (Merck, Germany) and HCl (Merck, Germany). Chromatographic analysis was performed using as a mobile phases acetonitrile (Merck, Germany) and triethylammonium acetate (TEAA, Merck, Germany). Finally, SPR analysis also used KCl and 4-(2-hydroxyethyl)-1-piperazineethanesulfonic acid (HEPES, Merck, Germany).

Instruments

The chromatographic system consisted of an Agilent 1100 Series HPLC instrument equipped with a G1311A quaternary pump, a G1379A degasser, a G1315B photodiode-array (PDA) detector furnished with a 13-µL flow cell and an Agilent Chemstation for data acquisition and analysis (Rev. A 10.02), all of them from Agilent Technologies (Waldbronn, Germany). Samples were injected with a Rheodyne 7725(i) (Cotati, CA, USA) injection valve equipped with a 20 µL sample loop. Samples were analyzed on a Clarity Oligo-RP column (50 mm × 4.6 mm i.d., particle size 2 µm) from Phenomenex (Torrance, CA, USA). Temperature of the column was kept at 25ºC using an HPLC column thermostat (GECKO 2000).

SPR experiments were performed on a four-channel Biacore T100 optical sensor instrument (BIAcore AB, Uppsala, Sweden). All experiments were performed on sensor chips SA (sensor chip with immobilized streptavidin) also obtained from BIAcore.

Molecular absorption spectra between 220 and 700 nm were recorded with an Agilent HP8453 diode array spectrophotometer. Temperature was controlled with a 89090A Agilent peltier device. CD spectra between 220 and 700 nm were recorded with a Jasco (Tokyo, Japan) J-810 spectropolarimeter equipped with a Julabo (Seelbach, Germany)

F-25/HD temperature control unit. Hellma® quartz cuvettes (path length of 1.0 cm, 1500 μl or 3000 μl volume) were used.

A Cyberscan 2500 pH meter from Eutech Instruments (Singapore) with an Orion SA 720 pH/ISE meter and micro combination pH electrode (Thermo, USA) was used for pH measurement of samples and buffers.

Procedure

Chromatographic analysis of TBA and / or TmPyP4 samples was performed using a typical mobile phase for oligonucleotide analysis. Therefore, a binary gradient based on 0.1 M TEAA as aqueous solution (channel A) and acetonitrile as organic modifier (channel B) has been used. The total flow-rate was set to 1 mL min^{-1}. The following gradient was used: 0 min (95 % A), 2.5 min (90 % A), 5 min (80 % A), 7.5 min (60 % A), 8.5 min (35 % A), 9.5 min (100 % A), 10.5 min (95 % A) and, finally, 13 min (95 % A). Photodiode Array Detection (PDA) was performed between 220 and 700 nm. First, a chromatogram of a TBA sample (40 μM) was recorded. Next, samples with different C_{TmPyP4}:C_{TBA} ratios were injected. In all cases, C_{TBA} was fixed to 40 μM and C_{TmPyp4} was accordingly modified. Finally, a chromatogram of a TmPyP4 sample (80 μM) was measured. The pH of the injected samples was 6.8.

In SPR experiments, 5'-biotin labelled DNA was immobilized in three flow cells, while a fourth cell was left blank as control. The SPR experiments were performed at 20 ºC in filtered, degassed, 1 mM HEPES buffer (pH 7.4) containing 100 mM KCl. TmPyP4 solutions were prepared by serial dilutions in a concentration range from 10 nM to 15 μM. Parameters for each analyte injection were: flow, 15 μl/min; contact time, 60 s (time enough to arrive to the steady-state region); and dissociation time, 250 s. Finally, a set of sensorgrams at different C_{TmPyP4} values was obtained.

Spectroscopic analysis of the interaction of TBA and porphyrin was carried out by two types of experiments. In all cases, molecular absorption and CD spectra were acquired at each temperature or C_{TmPyP4}:C_{TBA} ratio.

Mole-ratio experiments were done by addition of small volumes of TmPyP4 stock solution to an oligonucleotide solution (volume, 2.5 ml; C_{TBA}, 3.0 μM). Experimental conditions for these experiments were 25 ºC, pH 6.8 and 150 mM ionic strength (6 mM Na_2HPO_4, 10 mM KH_2PO_4, 111 mM KCl, 1 mM $MgCl_2$). Mole-ratio experiments were monitored *in situ*, taking advantage of the stirrer incorporated at the cell holder of the Agilent and Jasco J-810 instruments.

Melting experiments were carried out stepwise at 1 ºC increments from 20 to 80 ºC with a temperature rate of 0.5 ºC/min and 90 s of thermal stabilization. Each sample was initially stabilized at the starting temperature for 15 min. C_{TBA} and C_{TmPyP4} were 3 and 4.5 μM, respectively. Melting experiments were also carried out at pH 6.8 and 150 mM ionic strength.

Data analysis

SPR data were analyzed using the BIAevaluation 4.01 software. Spectroscopic data recorded along HPLC-PDA runs and melting and mole-ratio experiments were analyzed using two different chemometric methods: Equispec [21] and Multivariate Curve Resolution by Alternating Least Squares (MCR-ALS, [22]). In both cases, the goal of the analysis was the calculation of the concentration profiles (which are related to the stoichiometry and to the equilibrium constants), and the pure spectra or chromatogram for each one of the three species involved in the studied equilibria (TBA, TmPyP4 and the interaction complex).

The Equispec program was applied for the analysis of data recorded along *in situ*-monitored mole-ratio experiments. The calculated concentration profiles were constrained to fulfil a previously postulated chemical model defined by (i) a set of

stoichiometries for the proposed species, (ii) the fulfilment of mass-action law, and (iii) approximate values of their equilibrium constants. In this work, the equilibrium constant (log β) calculated from application of Equispec refers to the following equilibrium:

TmPyP4 + TBA ↔ Complex

Multivariate Curve Resolution by Alternating Least Squares (MCR-ALS) is a procedure based on Factor Analysis methods [23] that can be applied to analyze spectroscopic data recorded along a biochemical or biophysical process without the previous postulation of a physicochemical model [24-26]. In this work, spectroscopic data recorded along HPLC runs and melting experiments were analyzed using MCR-ALS because, in these cases, it was not possible to postulate a simple physicochemical model to describe the monitored equilibria. For HPLC-PDA, absorbance data recorded along each run were arranged in a table with *t* rows (corresponding to *t* retention times at which spectra were measured) and *w* columns (corresponding to the *w* wavelengths at which absorbance were measured) (Scheme 2). This table or data matrix was next unfolded into a vector, with dimensions 1 x *w***t*. For a set of *c* HPLC-PDA runs corresponding to *c* different samples, the set of unfolded vectors builds up a new data matrix **D**, the size of which is *c* rows (number of acquired chromatograms) and *w***t* columns. MCR-ALS analysis was then applied to analyze this data matrix **D**, allowing the calculation of the concentration profiles, as well as the unfolded pure chromatograms (1 x *w***t*) for each one of the considered species. These unfolded pure chromatograms were finally folded to recover the pure chromatograms with dimensions *w* x *t*, i.e., the same dimensions as the original data matrix. Analysis of melting data has been explained elsewhere [24-26]. All MCR-ALS calculations were performed using in-house MATLAB (version 7, The Mathworks Inc, Natick, MA) routines (Codes are freely available at the electronic address: www.ub.edu/mcr).

Results and Discussion

HPLC-PDA data

HPLC-PDA runs of TBA, TmPyP4 and their mixtures were monitored from 220 to 700 nm. With the goal of simplicity, only those chromatograms acquired at 422 nm (wavelength at which the absorbance of TmPyP4 reaches a maximum) are shown in Figure 1. As expected, TBA can not be detected at this wavelength. However, at 260 nm a broad signal could be observed (see inset), which reflects the complex structure of TBA at the experimental conditions. Panels 1B-E show the chromatograms recorded for several mixtures at different C_{TmPyP4}:C_{TBA} ratios. Finally, panel 1F shows the chromatogram for a TmPyP4 sample. The presence of two peaks in the chromatogram of TmPyP4 sample is striking, and it could be related to the existence of a mixture of porphyrin species. This mixture could be due to the existence of a large impurity, a possible degradation of the solid reagent or the stock solution, or the existence of a equilibrium. The frist two possibilities have been ruled out on the basis of the measured UV-visible spectra (Fig. 1G) for the two peaks and of the measured NMR and MS spectra (see Supplementary Material). Therefore, the existence of an equilibrium between two forms of TmPyP4 should not be discarded. An acid– base equilibrium does not seem to be the reason for this second peak because this kind of equilibria would produce smeared peaks. Other explanations, such as the existence of a monomer–dimer equilibrium, do not seem to be acceptable because NMR studies of porphyrin self-association in solution have shown that aggregation or dimerization effects are not significant at concentrations up to 1 mM [27]. These studies, however, did not take into account the possible effects related to the stationary phase in HPLC studies.

Absorbance data recorded along HPLC-PDA runs were analyzed with MCR-ALS. Figure 2A shows the whole data set recorded along the HPLC run corresponding to a mixture containing 40 μM TBA and 80 μM TmPyP4. This data set was unfolded into a vector, according to Scheme 2. A similar procedure was applied to all others data sets recorded for TBA and mixtures. A matrix **D** was then built up by merging the vectors

corresponding to all HPLC-PDA runs. Finally, MCR-ALS analysis of matrix **D** allowed the calculation of the concentration profiles and pure chromatograms for each one of the three species considered. From the calculated concentration profiles (Figure 2b), it was proposed the formation of 1:1 TmPyP4:TBA complex. Again, with the goal of simplicity, only those pure chromatograms calculated at 422 nm are shown (Figure 2c). As observed experimentally, whereas TBA does not show any signal at this wavelength, TmPyP4 shows two peaks at 3.9 and 6.1 minutes. The resolved chromatogram for the interaction complex shows also two peaks. Whereas the second peak appears at the same retention time as the second peak of TmPyP4 (6.1 minutes), the first peak shows a shift up to 5 minutes.

In situ-monitored mole-ratio experiments

The molecular absorption spectrum of TBA is typical for a DNA, showing an absorbance maximum around 260 nm (Figure 3a). More interesting is its CD spectrum, showing positive bands at 293 and 244 nm and a negative band at 268 nm, which are typical signatures for an antiparallel G-quadruplex structure formed in the presence of K^+ ions (Figure 3b) [28]. On the addition of TmPyp4, molecular absorption spectra showed the apparition of a new band at 430 nm. Free TmPyP4 shows an intense band at 422 nm. Therefore, the apparition of this band at 430 nm reflects the existence of some interaction between TBA and the porphyrin. At higher C_{TmPyP4}:C_{TBA} ratios the band at 430 nm shifted to 423 nm, which indicates the presence of free TmPyP4 in solution. TmPyP4 does not show any CD signal between 220 and 550 nm. Hence, spectral changes observed in Figure 3b upon addition of TmPyP4 are solely related to modifications in TBA structure. Interaction of TmPyP4 with the G-quadruplex structure produces a slight decrease of the positive band at 292 nm and a small shift and decrease of the bands at 263 nm and 244 nm.

Molecular absorption and CD data sets were merged into a data matrix **D**. Analysis of this data matrix with the Equispec program allowed the calculation of the concentration

profiles and pure spectra for the three species considered. The best fit was achieved when a 1:1 stoichiometry was considered (log K = 5.7 ± 0.2). The calculated concentration profiles (Figure 3c) are quite similar to those obtained from the HPLC-based mole ratio experiment (Figure 2B). The calculated molecular absorption (Figure 3d) and CD (Figure 3e) spectra give information about the nature of the interaction between TBA and TmPyP4. Hence, hypochromism and red shift in the visible band of the ligand clearly denotes an intercalation process [2]. The calculated CD spectrum for the interaction complex resembles quite well that of the initial G-quadruplex, despite the disappearance of the negative and positive bands at 270 and 240 nm, respectively.

The loss of the negative band around 270 nm has been explained by an incomplete formation of the G-quadruplex structure, which is now distinct from the case in the sole presence of K^+ ions [28]. This incomplete formation could be due to the intercalation of the ligand into the G-quadruplex structure.

Biospecific Interaction Analysis

After immobilization of the biotin-labelled TBA on the SA chip, injection of a series of TmPyP4 solutions was carried out. Figure 4a shows the experimental sensorgrams obtained in one of these series. At low C_{TmPyP4}, DNA binding sites are not saturated at the end of the porphyrin injection, as denoted by the absence of a plateau. At higher C_{TmPyP4}, the response achieves a plateau, which denotes a fast binding process. Figure 4b shows the results obtained after fitting the response versus C_{TmPyP4} (affinity analysis). The calculated log K value using a steady state model was 5.1 ± 0.2, which agrees quite well with the value previously calculated from the molecular absorption and CD data. The calculated value for chi^2 parameter was 56.0, which indicated a relative good fit of the experimental data to the postulated 1:1 interaction model.

Melting experiments

Thermal denaturation experiments give information about the relative stability of DNA structures upon ligand binding. In our case, melting experiments were carried out to have additional information about the influence of TmPyP4 on the stability of G-quadruplex TBA structure.

Figure 5 shows the melting profiles at 295 nm for TBA and for two TmPyP4:TBA mixtures [29]. TBA shows a single transition with a melting temperature of 48 ± 1 ºC. The presence of a unique transition indicates the unfolding of the G-quadruplex in an all-or-none process. Upon addition of TmPyP4, melting profiles still show a unique transition with melting temperatures 50 (C_{TmPyP4}:C_{TBA} ratio = 0.5) and 55 ^{o}C (C_{TmPyP4}:C_{TBA} ratio = 1.0). The observed shift of the melting temperatures upon ligand binding denotes a relative higher affinity of the ligand for the G-quadruplex structure than for the unfolded TBA.

The interaction of small organic ligands with G-quadruplexes has been a matter of research since the discovery of these DNA structures *in vivo*. This research has focused on different types of molecules, as can be seen in the recent review from Monchaud and Teulade-Fichou [30]. Despite the variety of ligands that bind the G-quadruplex structure, natural porphyrins and their synthetic derivatives are among those studied most extensively. However, to our knowledge, little work has been done in the study of the interaction between porphyrins and the intramolecular G-quadruplex adopted by TBA [12,31]. Recently, the potential role of porphyrins as a modulate agent of TBA aptamer in blood clotting was proposed [12]. In the current work, it is concluded that TBA and TmPyP4 form a 1:1 complex with a weak binding at 25 ºC (log K = 5.7 ± 0.1). The determined stoichiometry and the calculated log K value are similar to those described by Haq and coworkers (a 1:1 complex with a log K = 5.3 ± 0.1) from analysis of isothermal titration calorimetry and optical data in slightly different experimental conditions (10mM KH_2PO_4/K_2HPO_4, 200 mM KCl, 0.1 mM EDTA) [31]. In contrast, the calculated value in the current work is lower than the value determined by Joachimi and coworkers (log K = 6.5 ± 0.1) in predominantly Na^+ buffer conditions (1x phosphate-

buffered saline [PBS], 137 mM Na^+, and 3 mM K^+, pH 7.4) [12]. It should be taken into account, however, that the comparison of the log *K* values between predominantly K^+ solutions and predominantly Na^+ solutions fails to take into account not only changes in the ionic strength but also differences in the structure and stability of TBA G-quadruplex in different salts [28,32]. Because of this, it is rather uncertain to extract any conclusion from the comparison of log *K* values in the different K^+-containing buffers apart from the apparent weak binding that could be related to the partial folding of TBA at this temperature.

Finally, it should be mentioned that the intercalative binding mode is still a subject of controversy. Based on experimental data and dynamic molecular modelling simulations, Haq and coworkers pointed to the binding of TmPyp4 by intercalation at the GpG site in TBA [31]. In this sense, the results presented in this work show that the G-quadruplex structure of TBA is partially distorted on interaction with TmPyp4, a fact that could denote an intercalative binding mechanism, rather than through either electrostatic interaction or end-stacking mode.

Acknowledgements

This research was supported by the grants CTQ2006-15052-C02-01/BQU, CTQ2007-28940-E/BQU, and BFU2007-63287/BMC from the Spanish *Ministerio de Educación y Ciencia*.

Figure Captions

Scheme 1. A) Antiparallel G-quadruplex structure of thrombin binding aptamer (TBA). B) Molecular structure of 5, 10, 15, 20-*tetraki*s-(*N*-methyl-4-pyridyl)-21,23H-porphyrin (TmPyP4).

Scheme 2. Unfolding procedure and MCR-ALS analysis of the absorbance data recorded along HPLC-PDA runs. Each HPLC-PDA run produces a data matrix which dimensions are *w* wavelengths and *t* retention times. Merging several data matrices corresponding to different runs produces a data cube with dimensions *w* x *t* x *c*. In order to analyze the data cube with MCR-ALS it is necessary a previous unfolding of the each data matrix into a vector with dimensions 1 x *w***t*. Merging all the vectors produces a data matrix **D**. Analysis of this data with MCR-ALS provides the calculated concentration profiles and the pure chromatogram for each one of the species considered. Finally, the resolved chromatograms must be folded again into the corresponding matrices with dimensions *w* x *t*. Nr., number

Figure 1. HPLC-PDA chromatograms at 422 nm for several samples containing different C_{TMPyP4}:C_{TBA} ratios. (A) TBA 40 μM (inset: Chromatogram obtained at 260 nm). (B) 0.5:1 ratio C_{TMPyP4}:C_{TBA}. (C) 1:1 ratio C_{TMPyP4}:C_{TBA} ratio. (D) 2:1 ratio C_{TMPyP4}:C_{TBA}. (E) 3:1 ratio C_{TMPyP4}:C_{TBA}. (F) 80 μM TmPyP4. (G) Spectra between 200 nm and 550 nm of the two resolved peaks in panel F. Solis line, first peak; dashed line, second peak. In all panels, ma.u. refers to miliabsorbance units.

Figure 2. a) HPLC-PDA data obtained for a sample with C_{TMPyP4}:C_{TBA} ratio = 2. In this case, *w* = 316, and *t* = 1943. b) Calculated concentration profiles from the MCR-ALS analysis of the whole set of HPLC-PDA data recorded for the free TBA, free TmPyP4

and for the mixtures. Dotted points, MCR–ALS resolved points; solid line, interpolated concentration profiles with the Curve Fitting Toolbox of MATLAB software. (C) Chromatograms at 422 nm for each of the proposed species. Blue, TBA; green, TmPyP4; red, interaction complex. In panels (A) and (C), ma.u. refers to miliabsorbance units. (For interpretation of the references of color in this figure legend, the reader is refered to the web version of this article.).

Figure 3. a) Molecular absorption spectra recorded along a mole-ratio experiment. b) CD spectra recorded along a mole-ratio experiment. c) Concentration profiles resolved with the Equispec program from the simultaneous analysis of the data depicted in panels a) and b). d) Pure resolved molecular absorption spectra. e) Pure resolved CD spectra. Blue: TBA; green: TmPyP4; red: interaction complex. In panels (a), a.u. refers to absorbance units. (For interpretation of the references of color in this figure legend, the reader is refered to the web version of this article.)

Figure 4. a) Experimental SPR data for the binding analysis of TBA and TmPyP4 at several C_{TmPyP4}. b) Affinity analysis of the experimental data.

Figure 5. Absorbance vs. temperature curves at 295 nm recorded along melting experiments. Blue: TBA sample; green, C_{TMPyP4}:C_{TBA} ratio = 0.5; red, C_{TMPyP4} : C_{TBA} ratio = 1.0. a.u., arbitrary units. (For interpretation of the references of color in this figure legend, the reader is refered to the web version of this article.)

Scheme 1.

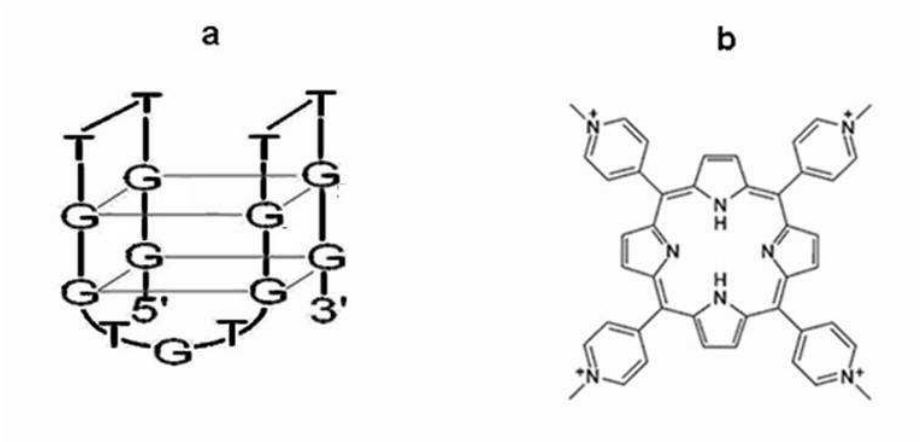

Scheme 2.

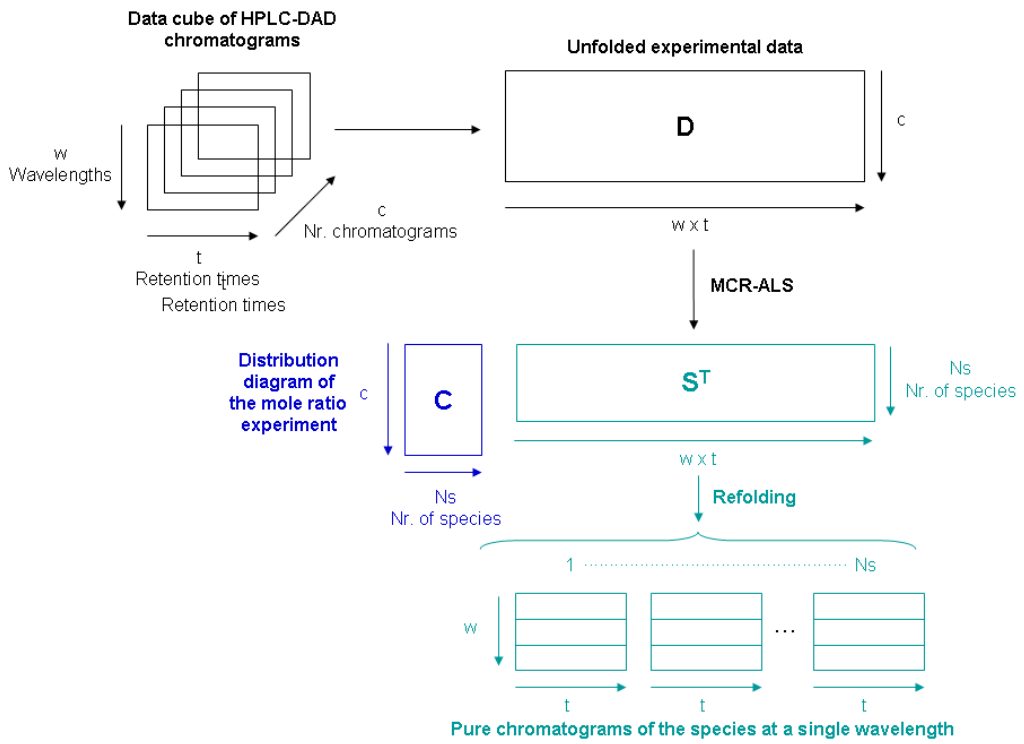
Data cube of HPLC-DAD chromatograms
w
Wavelengths
t
Retention times
c
Nr. chromatograms
Unfolded experimental data
D
c
w x t
MCR-ALS
Distribution diagram of the mole ratio experiment
c
C
Ns
Nr. of species
S^T
Ns
Nr. of species
w x t
Refolding
1
Ns
w
t
t
t
Pure chromatograms of the species at a single wavelength

Figure 1.

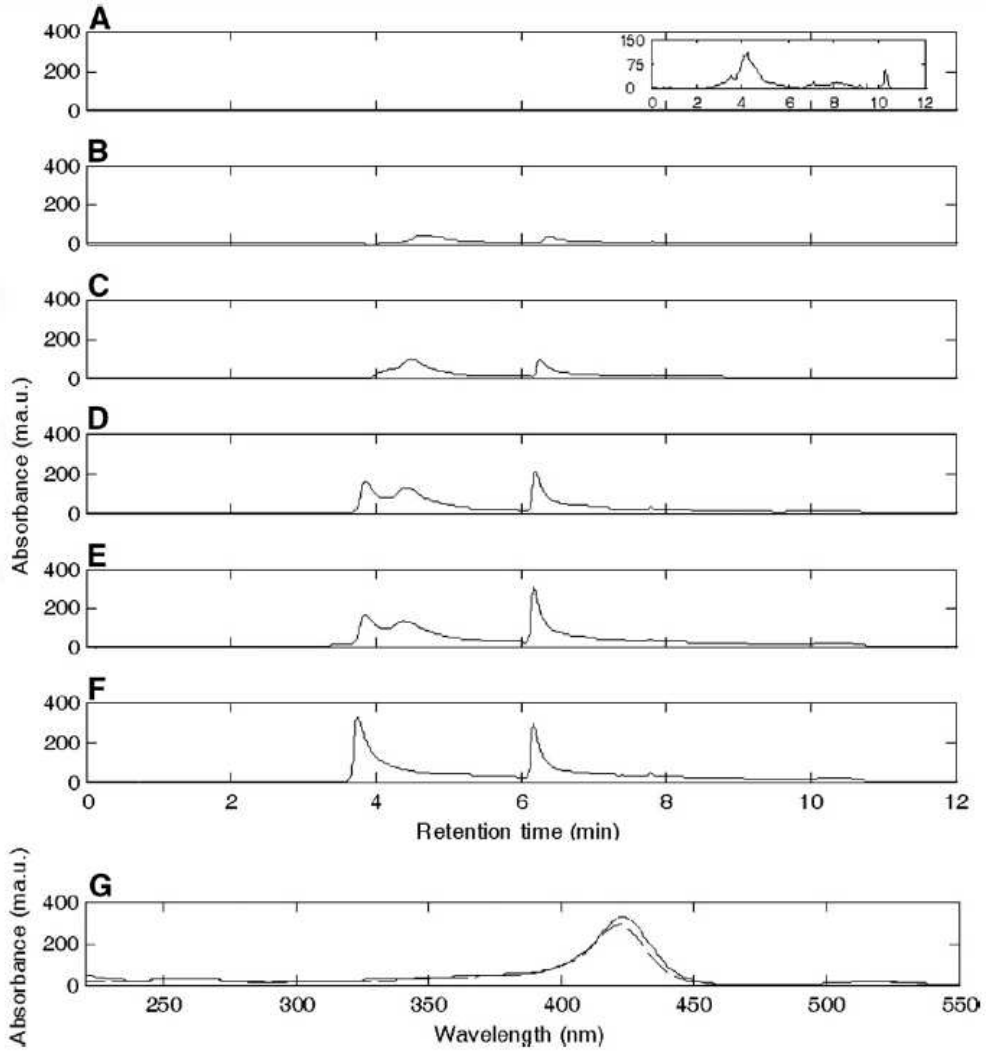
A
B
C
D
E
F
G
400
200
0
150
75
0
0
2
4
6
8
10
12
Absorbance (ma.u.)
Retention time (min)
250
300
350
400
450
500
550
Wavelength (nm)

Figure 2.

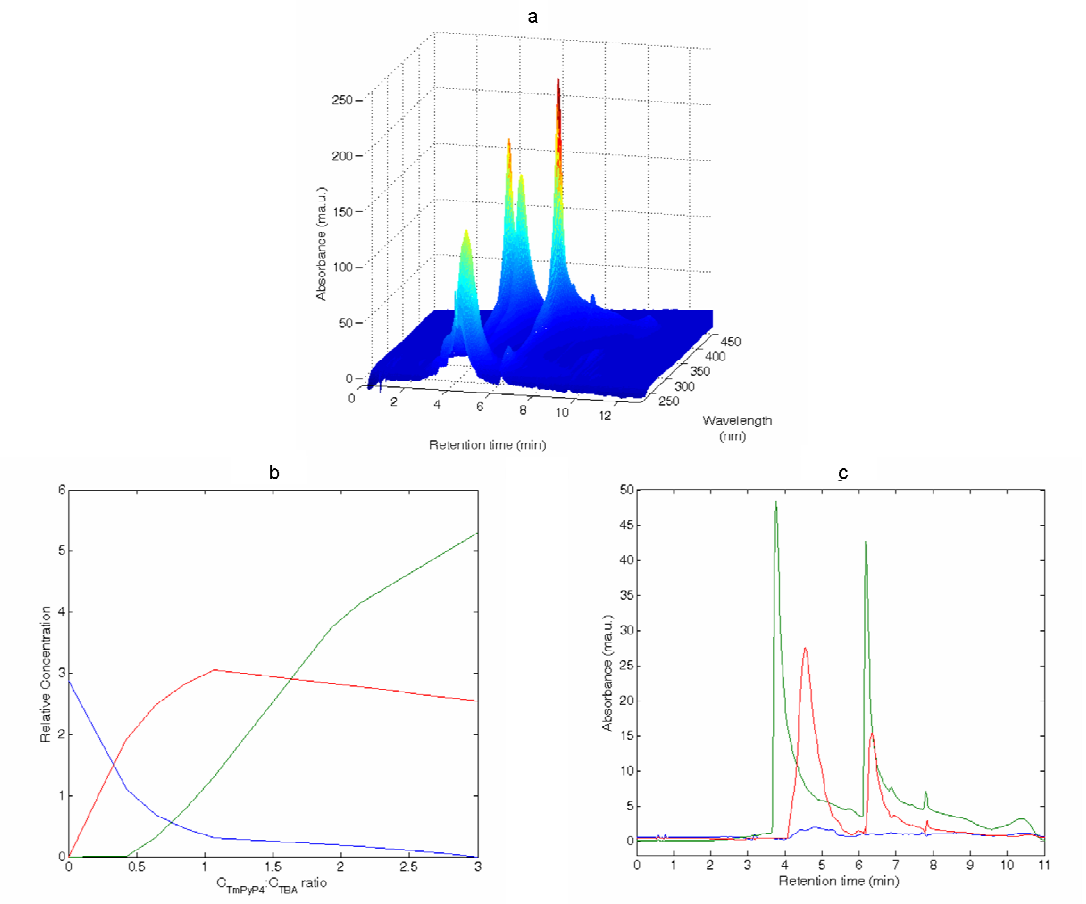
a
Absorbance (ma.u.)
250
200
150
100
50
0
0
2
4
6
8
10
12
Retention time (min)
450
400
350
300
250
Wavelength (nm)
b
Relative Concentration
0
1
2
3
4
5
6
0
0.5
1
1.5
2
2.5
3
C_TmPyP4:C_TEA ratio
c
Absorbance (ma.u.)
0
5
10
15
20
25
30
35
40
45
50
0
1
2
3
4
5
6
7
8
9
10
11
Retention time (min)

Figure 3.

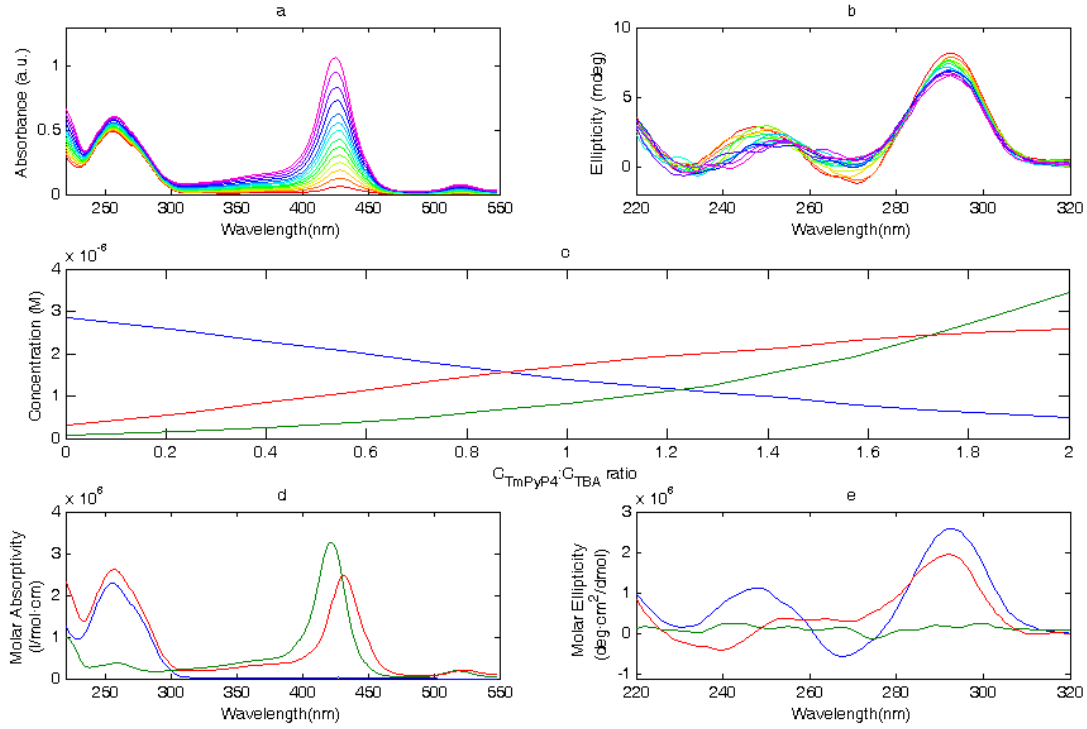
a
Absorbance (a.u.)
Wavelength(nm)
b
Ellipticity (mdeg)
Wavelength(nm)
c
x 10^-6
Concentration (M)
C_TmPyP4:C_TBA ratio
d
x 10^6
Molar Absorptivity (l/mol·cm)
Wavelength(nm)
e
x 10^6
Molar Ellipticity (deg·cm^2/dmol)
Wavelength(nm)

Figure 4.

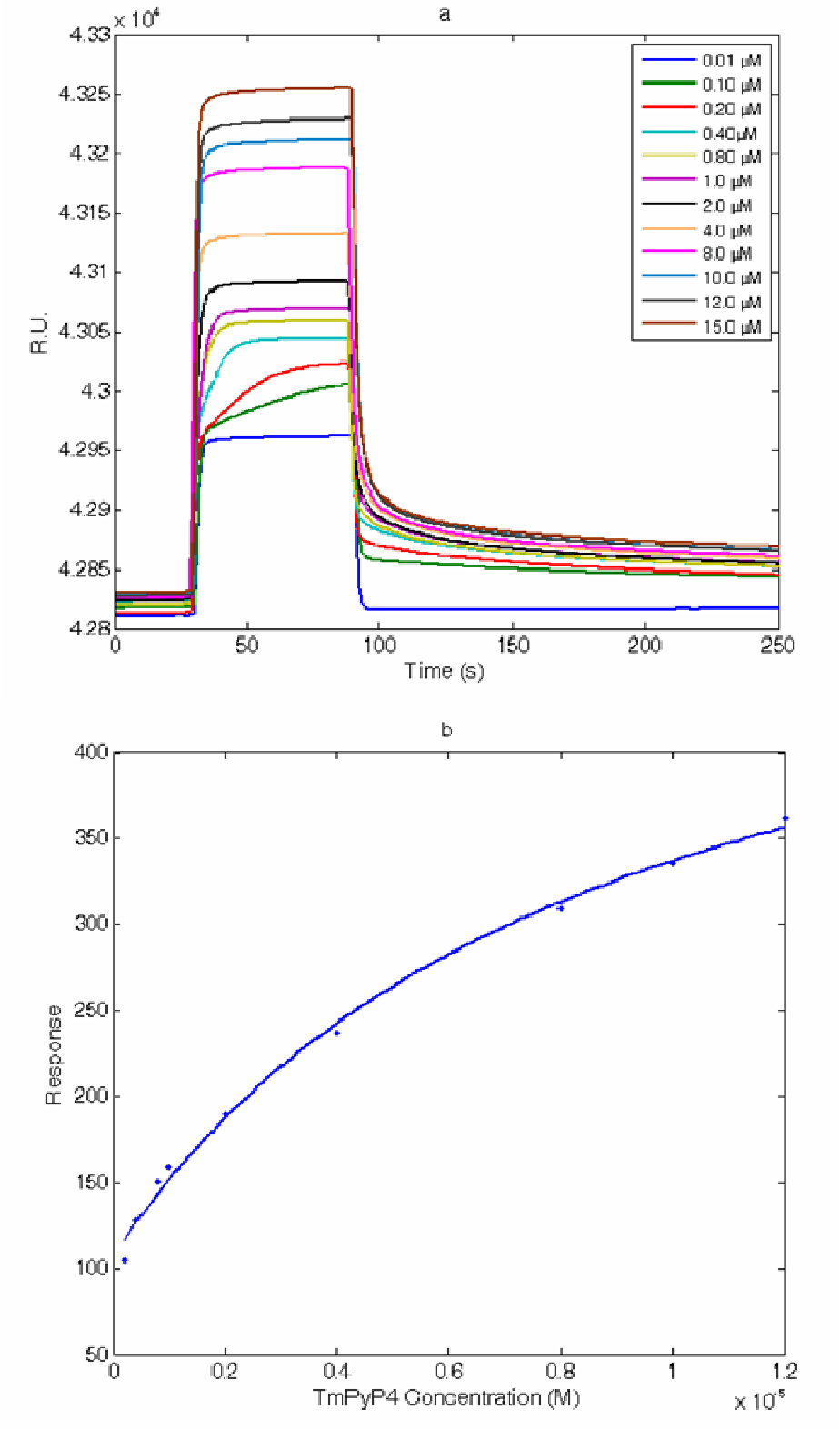
a
x 10^4
4.33
4.325
4.32
4.315
4.31
4.305
4.3
4.295
4.29
4.285
4.28
R.U.
0
50
100
150
200
250
Time (s)
0.01 µM
0.10 µM
0.20 µM
0.40µM
0.80 µM
1.0 µM
2.0 µM
4.0 µM
8.0 µM
10.0 µM
12.0 µM
15.0 µM
b
400
350
300
250
200
150
100
50
Response
0
0.2
0.4
0.6
0.8
1
1.2
TmPyP4 Concentration (M)
x 10^-5

Figure 5.

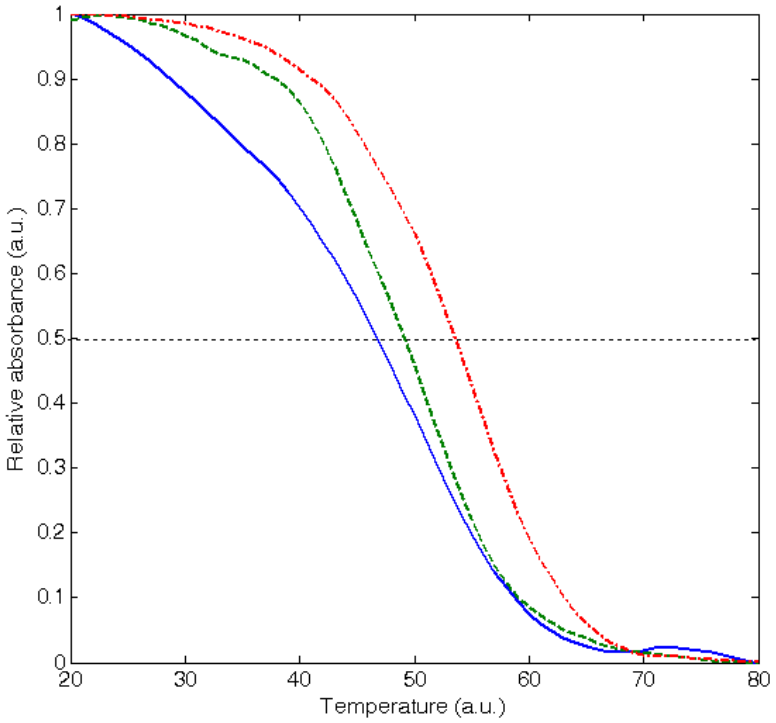
Relative absorbance (a.u.)
Temperature (a.u.)
0
0.1
0.2
0.3
0.4
0.5
0.6
0.7
0.8
0.9
1
20
30
40
50
60
70
80

References

[1] H. Fernando, A.P. Reszka, J. Huppert, S. Ladame, S. Rankin, A.R. Venkitaraman, S. Neidle, S. Balasubramanian, A conserved quadruplex motif located in a transcription activation site of the human c-kit oncogene, Biochemistry 45 (2006) 7854–7860.

[2] S. Neidle, S. Balasubramanian, Quadruplex Nucleic Acids, Royal Society of Chemistry, Cambridge, UK, 2006.

[3] A. Siddiqui-Jain, C.L. Grand, D.J. Bearss, L.H. Hurley, Direct evidence for a G-quadruplex in a promoter region and its targeting with a small molecule to repress c-MYC transcription, Proc. Natl. Acad. Sci. USA 99 (2002) 11593– 11598.

[4] G.F. Joyce, In vitro evolution of nucleic acids, Curr. Opin. Struct. Biol. 4 (1994) 331–336.

[5] A.D. Ellington, R. Conrad, Aptamers as potential nucleic acid pharmaceuticals, Biotechnol. Annu. Rev. 1 (1995) 185–214.

[6] J. Feigon, T. Dieckmann, F.W. Smith, Aptamer structures from A to zeta, Chem. Biol. 3 (1996) 611–617.

[7] K.Y. Wang, S. McCurdy, R.G. Shea, S. Swaminathan, P.H. Bolton, A DNA aptamer which binds to and inhibits thrombin exhibits a new structural motif for DNA, Biochemistry 32 (1993) 1899–1904.

[8] L.C. Bock, L.C. Griffin, J.A. Latham, E.H. Vermaas, J.J. Toole, Selection of single-stranded DNA molecules that bind and inhibit human thrombin, Nature 355 (1992) 564–566.

[9] R.F. Macaya, P. Schultze, F.W. Smith, J.A. Roe, J. Feigon, Thrombin-binding DNA aptamer forms a unimolecular quadruplex structure in solution, Proc. Natl. Acad. Sci. USA 90 (1993) 3745–3749.

[10] K. Padmanabhan, K.P. Padmanabhan, J.D. Ferrara, J.E. Sadler, A. Tulinsky, The structure of a-thrombin inhibited by a 15-mer single-stranded DNA aptamer, J. Biol. Chem. 268 (1993) 17651–17654.

[11] J.A. Kelly, J. Feigon, T.O. Yeates, Reconciliation of the X-ray and NMR structures of the thrombin-binding aptamer d(GGTTGGTGTGGTTGG), J. Mol. Biol. 256 (1996) 417–422.

[12] A. Joachimi, G. Mayer, J.S. Hartig, A new anticoagulant–antidote pair: Control of thrombin activity by aptamers and porphyrins, J. Am. Chem. Soc. 129 (2007) 3036–3037.

[13] J.J. Green, S. Ladame, L.M. Ying, D. Klenerman, S. Balasubramanian, Investigating a quadruplex–ligand interaction by unfolding kinetics, J. Am. Chem. Soc. 128 (2006) 9809–9812.

[14] R. Gambari, Biospecific interaction analysis (BIA) as a tool for the design and development of gene transcription modifiers, Curr. Med. Chem. Anticancer Agents 1 (2001) 277–291.

[15] D.P. Goncalves, S. Ladame, S. Balasubramanian, J.K. Sanders, Synthesis and G-quadruplex binding studies of new 4-N-methylpyridinium porphyrins, Org. Biomol. Chem. 4 (2006) 3337–3342.

[16] M. Malmqvist, Biospecific interaction analysis using biosensor technology, Nature 361 (1993) 186–187.

[17] M. Biesaga, K. Pyrzynska, M. Trojanowicz, Porphyrins in analytical chemistry: A review, Talanta 51 (2000) 209–224.

[18] C.K. Lim, J.M. Rideout, D.J. Wright, Separation of porphyrin isomers by high-performance liquid chromatography, Biochem. J. 211 (1983) 435–438.

[19] P. Macours, F. Cotton, Improvement in HPLC separation of porphyrin isomers and application to biochemical diagnosis of porphyrias, Clin. Chem. Lab. Med. 44 (2006) 1433–1440.

[20] E. Magi, C. Ianni, P. Rivaro, R. Frache, Determination of porphyrins and metalloporphyrins using liquid chromatography–diode array detection and mass spectrometry, J. Chromatogr. A 905 (2001) 141–149.

[21] R.M. Dyson, S. Kaderli, G.A. Lawrance, M. Maeder, A.D. Zunderbuhler, Second order global analysis: The evaluation of series of spectrophotometric titrations for improved determination of equilibrium constants, Anal. Chim. Acta 353 (1997) 381–393.

[22] R. Tauler, A. Smilde, B. Kowalski, Selectivity, Local rank, 3-way data analysis, and ambiguity in multivariate curve resolution, J. Chemometr. 9 (1995) 31– 58.

[23] E.R. Malinowski, D.G. Howery, Factor Analysis in Chemistry, John Wiley, New York, 2002.

[24] J. Jaumot, M. Vives, R. Gargallo, Application of multivariate resolution methods to the study of biochemical and biophysical processes, Anal. Biochem. 327 (2004) 1–13.

[25] J. Jaumot, N. Escaja, R. Gargallo, C. Gonzalez, E. Pedroso, R. Tauler, Multivariate curve resolution: A powerful tool for the analysis of conformational transitions in nucleic acids, Nucleic Acids Res. 30 (2002) e92.

[26] S. Navea, A. de Juan, R. Tauler, Detection and resolution of intermediate species in protein folding processes using fluorescence and circular dichroism spectroscopies and multivariate curve resolution, Anal. Chem. 74 (2002) 6031–6039.

[27] K. Kano, H. Minamizono, T. Kitae, S. Negi, Self-aggregation of cationic porphyrins in water: Can pi–pi stacking interaction overcome electrostatic repulsive force?, J Phys. Chem. A 101 (1997) 6118–6124.

[28] S. Nagatoishi, Y. Tanaka, K. Tsumoto, Circular dichroism spectra demonstrate formation of the thrombin-binding DNA aptamer G-quadruplex under stabilizing cation-deficient conditions, Biochem. Biophys. Res. Commun. 352 (2007) 812–817.

[29] J.L. Mergny, A.T. Phan, L. Lacroix, Following G-quartet formation by UV-spectroscopy, FEBS Lett. 435 (1998) 74–78.

[30] D. Monchaud, M.P. Teulade-Fichou, A hitchhiker's guide to G-quadruplex ligands, Org. Biomol. Chem. 6 (2008) 627–636.

[31] I. Haq, J.O. Trent, B.Z. Chowdhry, T.C. Jenkins, Intercalative G-tetraplex stabilization of telomeric DNA by a cationic porphyrin, J. Am. Chem. Soc. 121 (1999) 1768–1779.

[32] V.M. Marathias, P.H. Bolton, Determinants of DNA quadruplex structural type: Sequence and potassium binding, Biochemistry 38 (1999) 4355–4364.

SUPPLEMENTARY MATERIAL

NMR spectrum of TmPyP4 (pH 6.8, 10 mM sodium phosphate buffer, 25 ºC). NMR spectrum was acquired in a Bruker Advance spectrometer operating at 800 MHz and equipped with a crioprobe. Water suppression was achieved by the inclusion of a WATERGATE module in the pulse sequence prior to acquisition.

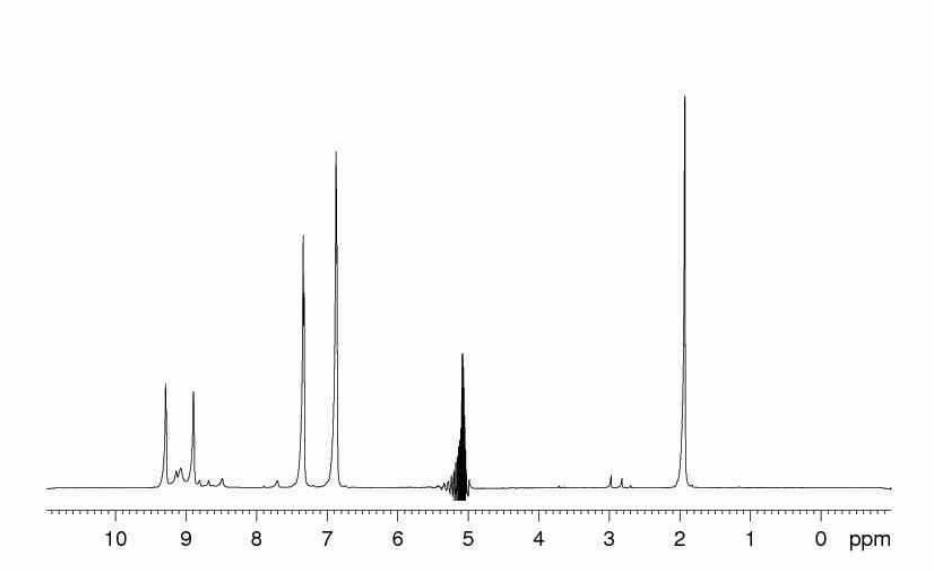

ESI(+)-MS spectrum of TmPyp4 (Experiments were run by direct injection using a positive electrospray ionisation mode applying a source voltage of 215 V in 1:1 mixture of H_20:CH_3CN)